Print ISSN : 0022-2755
Journal of Mines, Metals and Fuels
Contents available at: www.informaticsjournals.com/index.php/jmmf

Non-uniform Temperature Gradients Impact on Rayleigh-Darcy Convection: A Composite System with Couple Stress Fluid

R Sumithra[1], T Arul Selvamary[2*], and Shivaraja J. M[3]

[1]Associate Professor, [2, 3]Research Scholar Department of UG, PG Studies and Research in Mathematics, Government Science College (Autonomous), Nrupathunga University, Nrupathunga Road, Bengaluru-560 001, Karnataka, India. e-mail: arulthomasjt@gmail.com*

Abstract

The impact of non-uniform temperature gradients on Rayleigh-Darcy convection in a composite system of couple stress fluid is discussed. The composite system is bounded by stress-free surfaces and adiabatically insulated, and the fluid-porous layers are coupled by employing appropriate interfacial boundary conditions. To determine the eigen value, the regular perturbation method is used. The effect of dimensionless parameters on Rayleigh-Darcy convection is analysed graphically, and it is demonstrated that the couple stress parameter and couple stress viscosity ratio stabilise the system, while the opposite effect is observed for the Darcy number and thermal diffusivity ratio.

Keywords: *Rayleigh-Darcy Convection, Couple stress fluid, Composite system, Non-uniform temperature gradient.*

1. Introduction

Composite layers are formed by combining fluid and porous layers. The issue of heat convection in the composite layer is encountered in a number of technical, medicinal, and ecological applications. Buoyancy-driven convection in the composite layer has a variety of technical applications, including geothermal reservoirs, grain storage, subsurface pollution transport, and heat removal in nuclear power plants, to name a few. Convective heat transfer in Newtonian fluid layer with an overlaying porous layer was the focus of early composite layer research. A comprehensive literature evaluation of linear and non-linear convections in a fluid-saturated porous layer is presented in Nield and Bejan's [1] book. Sun [2] investigated the start of convection when a fluid layer above a saturated porous layer is heated from below. Many authors have investigated linear and non-linear composite layer stability analysis [3-11]. According to a linear stability study, the critical Rayleigh number in a porous medium decreases continuously as the thickness ratio between the fluid and the porous layer increases. Beaver-Joseph [12] established slip conditions at the porous-fluid interface, while Ochoa-Tapia and Whitaker [13] introduced momentum transfer at the contact. [14-15] have also investigated the fluid-porous interface boundary conditions. Sumithra and Manjunatha [16] studied parabolic and inverted parabolic temperature profiles in a composite layer. Sumithra*et al*. [17] studied Benard Marangoni convection in a porous fluid layer. They studied source-sink temperature gradients.

*Corresponding author

The Stokes [18] theory is the simplest extension of the classical fluid theory that allows for polar phenomena, such as an anti-symmetric stress tensor, couple stresses, and body couples. Couple stress is likely in fluids containing extra molecules. Couple stress fluids include synthetic lubricants, colloidal fluids, liquid crystals, and bio-fluids. Couple stress fluid's technical uses include, to name a few, lubrication concerns with squeezing film bearings, thrust bearings, and journal bearings. [19-23] employ the Darcy model and the Beavers- Joseph velocity slip at the porous media/fluid layer interface to characterise the flow in a porous medium. Siddeshwar and Pranesh [24] have explored both linear and nonlinear Boussinesq–Stokes convection. Shivakumara [25] investigated convection in a fluid-saturated porous media with non-uniform temperature gradients. Sumithra and Selvamary [26] revealed, when analysing surface tension-driven fluid convection in a composite layer, that the couple stress parameter serves as a system stabiliser.

This research aims to investigate the effects of beated from below temperature gradient (HTG), cooled from above temperature gradient (CTG) and step function temperature gradient on Rayleigh-Darcy convection (DRC) in couple stress fluid.

2. Mathematical formulation

Consider couple stress fluid flow in a height-bounded 2D composite system with free surfaces on both sides. The origin of the Cartesian coordinate system is created at the middle of the composite layer; from this point, the horizontal x-axis and vertical z-axis are derived. A fluid layer occupies Region 1, whereas a porous layer saturated with fluid occupies Region 2. The composite system's lower and upper free surfaces are kept at different constant temperatures T_l and T_u respectively, with $T_l > T_u$. In addition, gravity $\vec{g}$ exerts a downward force in a vertical direction. In fluid layer, the Navier-Stokes equation describes the flow of fluid with couple stress, whereas the Darcy equation governs the flow of the same fluid in porous layer.

The conservation of mass, momentum, energy, and the equation of state of the Region 1 are:

$$\nabla \cdot \vec{q}_1 = 0 \quad \text{... [1]}$$

$$\rho_0\left(\frac{\partial \vec{q}_1}{\partial t} + \left(\vec{q}_1 \cdot \nabla\right)\vec{q}_1\right) = -\nabla P_1 - \rho_0\left(1-\alpha_1\left(T_u - T_0\right)\right)\vec{g} + \mu\nabla^2\vec{q}_1 - \mu_1'\,\nabla^4\vec{q}_1 \quad \text{... [2]}$$

$$\frac{\partial T_1}{\partial t} + \left(\vec{q}_1 \cdot \nabla\right)T_1 = \kappa_1\nabla^2 T_1 \quad \text{... [3]}$$

The mass, momentum, energy, and equation of state of Region 2 are as follows:

$$\nabla \cdot \vec{q}_2 = 0 \quad \text{... [4]}$$

$$\frac{\rho_0}{\varphi}\frac{\partial \vec{q}_2}{\partial t} = -\nabla P_2 - \rho_0\left(1-\alpha_2\left(T_l - T_0\right)\right)\vec{g} - \frac{\mu}{K}\vec{q}_2 + \frac{\mu_2'}{K}\nabla^2\vec{q}_2 \quad \text{... [5]}$$

$$\mathrm{E}\frac{\partial T_2}{\partial t} + \left(\vec{q}_2 \cdot \nabla\right)T_2 = \kappa_2\nabla^2 T_2 \quad \text{... [6]}$$

Here denotes velocity, pressure, gravitational force, viscosity, couple-stress fluid viscosity, temperature, density, coefficient of thermal expansion, porosity, permeability, specific heat and ratio of heat capacities. denotes Laplacian operator, ρ_0 denotes density at a reference temperature, The subscripts 1 and 2 refer to fluid and porous regions respectively. Here $\vec{q}$ (u, v, w), P, $\vec{g}$, μ, μ', T , κ , ρ, α, ϕ, K, C_p, E denoted velocity, pressure, gravitational force, viscosity, couple-stress fluid viscosity, temperature, density, coefficient of thermal expansion, porosity, permeability, specific heat, and heat capacity ratio. $\nabla^2 = \frac{\partial^2}{\partial x^2} + \frac{\partial^2}{\partial y^2} + \frac{\partial^2}{\partial z^2}$ denotes Laplacian operator, ρ_0 denotes density at a reference temperature $T = T_0$, suffix 1 and 2 denotes fluid and porous regions respectively. Assuming that the fundamentally stable state of the composite system is quiet, the temperature distributions are determined to be

$$T_{1b}(z_1) = T_0 - \left(\frac{T_0 - T_u}{h_1}\right) z_1 \qquad 0 \le z_1 \le h_1 \qquad \text{... [7]}$$

$$T_{2b}(z_2) = T_0 - \left(\frac{T_l - T_0}{h_2}\right) z_2 \qquad -h_2 \le z_2 \le 0 \qquad \text{... [8]}$$

Here, $T_0 = \dfrac{\kappa_1 h_2 T_u + \kappa_2 h_1 T_l}{\kappa_1 d_2 + \kappa_2 h_1}$ represents the temperature of the interface, whereas the suffix b denotes the basic state. Insignificant perturbations are applied as q^*, P^*, θ^*, and ρ^* for velocity, pressure, temperature, and density for the goal of testing the stability of the fundamental solution. The perturbations caused by the quantities represented by asterisks are insignificant; consequently, it can be substituted in the equations (1)–(6) and curl are used twice to eliminate the pressure term from Equations (2) and (5). The variables are then functionally non-dimensionalised and expressed h_1, h_1^2/κ_1, κ_1/h_1 and $T_0 – T_u$ as the units of length, time, velocity, and temperature in the fluid layer and h_2, h_2^2/κ_2, κ_2/h_2 and $T_1 – T_0$ as the equivalent characteristic values in the porous layer. The non-dimensionalized equations of Region 1 and Region 2 are found with two unknowns w and θ two variables.

Assuming ω and θ are periodic waves, normal mode solutions may be expressed as

$$(w_1, \theta_1) = (W_1(z_1), \Theta_1(z_1))\, e^{i_1(l_1 x_1 + m_1 y_1) - \omega_1 t_1} \qquad \text{... [9]}$$

$$(w_2, \theta_2) = (W_2(z_2), \Theta_2(z_2))\, e^{i_2(l_2 x_2 + m_2 y_2) - \omega_2 t_2} \qquad \text{... [10]}$$

Here, ω is the frequency, and the wave number in x and y directions are denoted by l and m. Ordinary differential equations can be derived from non-dimensionalised partial differential equations by substituting the aforementioned formulae:

$$\left(C_p\left(D_1^2 - a_1^2\right)^3 - \left(D_1^2 - a_1^2\right)^2 - \frac{\omega_1}{\mathrm{Pr}_1}\left(D_1^2 - a_1^2\right)\right) W_1(z_1) = -R_c\, a_1^2\, \Theta_1(z_1) \qquad \text{... [11]}$$

$$\left(D_1^2 - a_1^2 + \omega_1\right)\Theta_1 = -W_1\, f_1(z_1) \qquad \text{... [12]}$$

$$\left(C_{p2}\left(D_2^2 - a_2^2\right)^2 - \left(D_2^2 - a_2^2\right) + \frac{Da\,\omega_2}{\mathrm{Pr}_2}\left(D_2^2 - a_2^2\right)\right) W_2(z_2) = R_{cp}\, a_2^2\, \Theta_2(z_2) \qquad \text{... [13]}$$

$$\left(D_2^2 - a_2^2 + \mathrm{E}\,\omega_2\right)\Theta_2 = -W_2\, f_2(z_2) \qquad \text{... [14]}$$

here, $D = \dfrac{d}{dz}$ denotes differential operator, $a_1^2 = \sqrt{l_1^2 + m_1^2}$ denotes wave number, $Da = \dfrac{K}{h_2^2}$ is the Darcy number, $C_p = \dfrac{\mu'}{\mu h_1^2}$, $\mathrm{Pr}_1 = \dfrac{\mu}{\rho_0 \kappa_1}$, $R_c = \dfrac{\rho_0\, g\, \alpha_1 (T_0 - T_u) h_1^3}{\mu \kappa_1}$ denotes couple stress parameter, prandtl number and Rayleigh number in fluid layer, $C_{p2} = \dfrac{\mu_2'}{\mu h_2^2}$, $\mathrm{Pr}_2 = \dfrac{\phi \mu}{\rho_0 \kappa_2}$, $R_{cp} = \dfrac{\rho_0\, g\, \alpha_2 (T_l - T_0) h_2^3}{\mu \kappa_2}$ denotes the above equivalent terms in porous layer. The relation between couple stress parameter in fluid and porous layers is expressed as $C_{p2} = \dfrac{\hat{h}}{\hat{\Lambda}} C_p$ and the relation between Rayleigh number in fluid and porous layer can be expressed as $R_{cp} = \dfrac{\hat{\alpha}_T\, Da\, \hat{\kappa}_T^2}{\hat{h}^4} R_c$.

We limit the analysis to stationary convection and use equations (11) to (14) to obtain the following equations, as the concept of exchange of stability applies in this process.

$$\left(C_p\left(D_1^2 - a_1^2\right) - 1\right)\left(D_1^2 - a_1^2\right)^2 W_1(z_1) = -R_c\, a_1^2\, \Theta_1(z_1) \qquad \text{... [15]}$$

$$\left(D_1^2 - a_1^2\right)\Theta_1 = -W_1\, f_1(z_1) \qquad \text{... [16]}$$

$$\left(C_{p2}\left(D_2^2-a_2^2\right)-1\right)\left(D_2^2-a_2^2\right)W_2\left(z_2\right)=R_{cp}\,a_2^2\,\Theta_2\left(z_2\right) \qquad \text{... [17]}$$

$$\left(D_2^2-a_2^2\right)\Theta_2=-W_2\,f_2\left(z_2\right) \qquad \text{... [18]}$$

The composite system's boundary conditions are as follows:

$$W_1(1)=0,\quad D_1^2\,W_1(1)=0,\quad D_1^4\,W_1(1)=0,\quad D_1\Theta_1(1)=0, \qquad \text{... [19]}$$

$$W_2\left(0\right)=0,\quad D_2^2\,W_2\left(0\right)=0,\quad D_2\,\Theta_2(0)=0, \qquad \text{... [20]}$$

$$\left.\begin{aligned} &W_1(0)=\frac{\hat{h}}{\hat{\kappa}_T}W_2(1),\ D_1W_1(0)=\frac{\hat{h}^2}{\hat{\kappa}_T}D_2W_2(1),\ (D_1^2+a_1^2)W_1(0)=\frac{\hat{h}^3}{\hat{\mu}\,\hat{\kappa}_T}\left(D_2^2+a_2^2\right)W_2(1),\\ &\left(D_1^4-a_1^4\right)W_1(0)=\frac{\hat{h}^5}{\hat{\Lambda}\,\hat{\kappa}_T}\left(D_2^4-a_2^4\right)W_2\left(1\right),\quad \Theta_1(0)=\frac{\hat{\kappa}_T}{\hat{h}}\Theta_2(1),\quad D_1\Theta_1(0)=D_2\,\Theta_2(1)\\ &\left(C_p\left(D_1^2-a_1^2\right)^2-D_1^2+3a_1^2\right)D_1W_1(0)=\frac{\hat{h}^4}{Da\,\hat{\kappa}_T}\left(1-C_{p2}\left(D_2^2-a_2^2\right)\right)D_2W_2(1) \end{aligned}\right\}. \qquad \text{... [21]}$$

Where, $\hat{\kappa}_T=\kappa_1/\kappa_2$ is the thermal diffusivity ratio, $\hat{\Lambda}=\mu_1'/\mu_2'$ is the couple-stress viscosity ratio, $\hat{\mu}=\mu_1/\mu_2$ viscosity ratio, and $\hat{\beta}=\alpha_1/\alpha_2$ thermal expansion coefficient ratio, and $\hat{h}=h_1/h_2$ depth ratio respectively.

3. Regular perturbation technique solution

The perturbation methods require the assumption of small parameters. At this point, we will use 'a_1' as the wavenumber, which is a very small number. The terms and are expanded sequentially, and then the set of terms with the same power in 'a_1' is solved until the answer is found.

$$\begin{bmatrix}W_1\\ \Theta_1\end{bmatrix}=\sum_{k=0}^{\infty}a_1^{2k}\begin{bmatrix}W_{1k}\\ \Theta_{1k}\end{bmatrix} \qquad \text{and} \qquad \begin{bmatrix}W_2\\ \Theta_2\end{bmatrix}=\sum_{k=0}^{\infty}\left(\frac{a_1}{\hat{h}}\right)^{2k}\begin{bmatrix}W_{2k}\\ \Theta_{2k}\end{bmatrix} \qquad \text{... [22]}$$

Eqs. (15) to (18) are solved using the composite system's boundary conditions to determine the velocities W_1 and W_2 of Region 1 and Region 2.

The equation's zero-order in a_1^2 solution is given by:

$$W_1\left(z_1\right)=0,\ W_2\left(z_2\right)=0,\ \Theta_1\left(z_1\right)=\frac{\hat{\kappa}_T}{\hat{h}},\quad \Theta_2\left(z_2\right)=1. \qquad \text{... [23]}$$

The first-order in a_1^2, Eqs. (15)–(18) then reduce to

$$D_1^6\,W_1\left(z_1\right)-\eta_1^2D_1^2\,W_1\left(z_1\right)+\frac{\hat{\kappa}_T}{\hat{h}}\eta_1^2\,R_c=0 \qquad \text{... [24]}$$

$$D_1^2\,\Theta_1-\frac{\hat{\kappa}_T}{\hat{h}}+W_1\,f_1\left(z_1\right)=0 \qquad \text{... [25]}$$

$$D_2^4\,W_2-\eta_2^2\,D_2^2\,W_2-\eta_2^2\,R_{cp}=0 \qquad \text{... [26]}$$

$$D_2^2\,\Theta_2-1+W_2\,f_2\left(z_2\right)=0 \qquad \text{... [27]}$$

The composite system's boundary conditions (19)-(21) reduces to

$$W_1(1)=D_1^2\,W_1(1)=D_1^4\,W_1(1)=D_1\,\Theta_1(1)=0, \qquad \text{... [28]}$$

$$W_2\left(0\right)=D_2^2\,W_2\left(0\right)=D_2\,\Theta_2(0)=0, \qquad \text{... [29]}$$

$$\left.\begin{aligned} &W_1(0)=\frac{1}{\hat{h}\,\hat{\kappa}_T}W_2(1),\quad D_1W_1(0)=\frac{1}{\hat{\kappa}_T}D_2W_2(1),\quad D_1^2W_1(0)=\frac{\hat{h}}{\hat{\mu}\,\hat{\kappa}_T}D_m^2W_2(1),\\ &D_1^4W_1(0)=\frac{\hat{h}^3}{\hat{\lambda}\,\hat{\kappa}_T}D_2^4W_2(1),\ \left(C_p D_1^5-D_1^3\right)W_1(0)=\left(\frac{\hat{h}^2}{Da\,\hat{\kappa}_T}\right)\left(D_2-C_{p2}D_2^3\right)W_2(1)\\ &\Theta_1(0)=\frac{\hat{\kappa}_T}{\hat{h}^3}\Theta_2(1),\quad D_1\Theta_1(0)=\frac{1}{\hat{h}^2}D_2\Theta_2(1) \end{aligned}\right\} \quad \text{... [30]}$$

Equation (24) and (26) has a general solution as:

$$W_1(z_1)=\left(\Psi_4+z_1\Psi_5+z_1^2\Psi_6+z_1^3\Psi_7+\mathrm{Cosh}(\eta_1 z_1)\Psi_8+\mathrm{Sinh}(\eta_1 z_1)\Psi_9+\frac{\hat{\kappa}_T}{24\hat{h}}z_1^4\right)R_c \quad \text{... [31]}$$

$$\eta_1^2=\frac{1}{C_p},\quad \eta_2^2=\frac{1}{C_{p2}},\ \Delta_1=\frac{\hat{\alpha}_T\,Da\,\hat{\kappa}_T^2}{\hat{h}^4},$$

$$W_2(z_2)=\left(z_2\Psi_2+\left(\frac{\mathrm{Cosh}(\eta_2 z_2)}{\eta_2^2}-\frac{1}{\eta_2^2}-\frac{z_2^2}{2}\right)\Delta_1+\mathrm{Sinh}(\eta_2 z_2)\Psi_1\right)R_{cp} \quad \text{... [32]}$$

where

$$\Psi_1=\frac{\left(O_{15}O_{16}-O_{13}O_{18}\right)}{\left(O_{14}O_{16}-O_{13}O_{17}\right)},\qquad \Psi_2=\frac{\left(O_{15}-O_{14}\Gamma_1\right)}{O_{13}},\qquad \Psi_3=\frac{\Delta_1}{\eta_2^2},$$

$$\Psi_4=\left(\frac{\Psi_2}{\hat{h}\hat{\kappa}_T}+O_{11}\Psi_1+O_{12}\right),\ \Psi_5=\left(\frac{\Psi_2}{\hat{\kappa}_T}+O_9\Psi_1+O_{10}\right),\qquad \Psi_6=\left(O_7\Psi_1+O_8\right),$$

$$\Psi_7=-\frac{\hat{h}^2\,\Psi_2}{6Da\,\hat{\kappa}_T}+O_5\Psi_1+O_6,\ \Psi_8=\left(O_1\Psi_1+O_2\right),\qquad \Psi_9=\left(O_3\Psi_1+O_4\right),$$

$$O_1=\frac{\hat{h}^3\eta_2^4}{\eta_1^4\,\hat{\Lambda}\,\hat{\kappa}_T}\mathrm{Sinh}(\eta_2),\quad O_2=\frac{\hat{h}^3\eta_2^2\Delta_1}{\eta_1^4\,\hat{\Lambda}\,\hat{\kappa}_T}\mathrm{Cosh}(\eta_2)-\frac{\hat{\kappa}_T}{\hat{h}\eta_1^4},$$

$$O_3=-\frac{\mathrm{Cosh}(\eta_1)}{\mathrm{Sinh}(\eta_1)}O_1,\quad O_4=-\left(\frac{\mathrm{Cosh}(\eta_1)}{\mathrm{Sinh}(\eta_1)}O_2+\frac{\hat{\kappa}_T}{\hat{h}\eta_1^4\,\mathrm{Sinh}(\eta_1)}\right),$$

$$O_5=\frac{\hat{h}^2\eta_2\,\mathrm{Cosh}(\eta_2)}{6Da\,\hat{\kappa}_T}\left(C_2\eta_2^2-1\right)-\frac{\eta_1^3\left(1-C_1\eta_1^2\right)}{6}O_3,$$

$$O_6=\frac{\hat{h}^2\Delta_1}{6Da\,\hat{\kappa}_T}\left(\frac{\mathrm{Sinh}(\eta_2)\left(C_2\eta_2^2-1\right)}{\eta_2}-1\right)-\frac{\eta_1^3\left(1-C_1\eta_1^2\right)}{6}O_4,$$

$$O_7=\frac{\hat{h}}{2\hat{\mu}\,\hat{\kappa}_T}\eta_2^2\,\mathrm{Sinh}(\eta_2)-\frac{\eta_1^2}{2}O_1,\quad O_8=\frac{\hat{h}}{2\hat{\mu}\,\hat{\kappa}_T}\left(\mathrm{Cosh}(\eta_2)-1\right)\Delta_1-\frac{\eta_1^2}{2}O_2,$$

$$O_9 = \frac{\eta_2}{\hat{\kappa}_T}\operatorname{Cosh}(\eta_2) - \eta_1 O_3,$$

$$O_{10} = \frac{\Delta_1}{\hat{\kappa}_T}\left(\frac{\operatorname{Sinh}(\eta_2)}{\eta_2} - 1\right) - \eta_1 O_4,$$

$$O_{11} = \frac{1}{\hat{h}\,\hat{\kappa}_T}\operatorname{Sinh}(\eta_2) - O_1,$$

$$O_{12} = \frac{\Delta_1}{\hat{h}\,\hat{\kappa}_T}\left(\frac{\operatorname{Cosh}(\eta_2) - 1}{\eta_2^2} - \frac{1}{2}\right) - O_2,$$

$$O_{13} = \frac{1}{\hat{h}\,\hat{\kappa}_T} + \frac{1}{\hat{\kappa}_T} - \frac{\hat{h}^2}{6Da\,\hat{\kappa}_T},$$

$$O_{14} = \left(O_{11} + O_9 + O_7 + O_5 + \operatorname{Cosh}(\eta_1) O_1 + \operatorname{Sinh}(\eta_1) O_3\right),$$

$$O_{15} = -\left(O_{12} + O_{10} + O_8 + O_6 + \operatorname{Cosh}(\eta_1) O_2 + \operatorname{Sinh}(\eta_1) O_4 + \frac{\hat{\kappa}_T}{24\,\hat{h}}\right),$$

$$O_{16} = -\frac{\hat{h}^2}{Da\,\hat{\kappa}_T},$$

$$O_{17} = \begin{pmatrix} 2O_7 + 6O_5 + \eta_1^2\ \operatorname{Cosh}(\eta_1) O_1 + \\ \eta_1^2\ \operatorname{Sinh}(\eta_1) O_3 \end{pmatrix},$$

$$O_{18} = -\begin{pmatrix} 2O_8 + 6O_6 + \eta_1^2\ \operatorname{Cosh}(\eta_1) O_2 + \\ \eta_1^2\ \operatorname{Sinh}(\eta_1) O_4 + \dfrac{\hat{\kappa}_T}{2\,\hat{h}} \end{pmatrix}$$

The following solvability condition is obtained by integrating equations (29) and (31) between $z = 0$ and $z = 1$, applying the pertinent boundary conditions, and adding the equation that is produced; this process produces the following result:

$$\int_0^1 W_1 f_1(z_1)\,dz_1 + \frac{1}{\hat{h}^2}\int_0^1 W_2 f_2(z_2)\,dz_2 = \frac{\hat{\kappa}_T}{\hat{h}} + \frac{1}{\hat{h}^2} \qquad \text{... [33]}$$

here, $f_1(z_1)$ and $f_2(z_2)$ take different forms according to the basic thermal gradients. We

denote $f_1(z_1) = \begin{cases} 1/\varepsilon & 0 \le z_1 \le \varepsilon \\ 0 & \varepsilon \le z_1 \le 1 \end{cases}$, and $f_2(z_2) = \begin{cases} 1/\varepsilon_m & 0 \le z_2 \le \varepsilon_m \\ 0 & \varepsilon_m \le z_2 \le 1 \end{cases}$ for HTG,

$f_1(z_1) = \begin{cases} 0 & 0 \le z_1 < 1-\varepsilon \\ 1/\varepsilon & 1-\varepsilon < z_1 \le 1 \end{cases}$ and $f_2(z_2) = \begin{cases} 0 & 0 \le z_2 \le 1-\varepsilon_m \\ 1/\varepsilon_m & 1-\varepsilon_m \le z_2 \le 1 \end{cases}$ for CTG,

$f_1(z_1) = f_1(\varepsilon)$ and $f_2(z_2) = f_2(\varepsilon_m)$ for STG.

Here are the equations for the critical Rayleigh numbers for HTG (R_{c1}), CTG (R_{c2}), and STG (R_{c3}) are in order.

$$R_{C1}=\frac{\frac{\hat{\kappa}_T}{\hat{h}}+\frac{1}{\hat{h}^2}}{\Omega_1+\Omega_2} \quad \text{... [34]}$$

$$R_{C2}=\frac{\frac{\hat{\kappa}_T}{\hat{h}}+\frac{1}{\hat{h}^2}}{\Omega_3+\Omega_4} \quad \text{... [35]}$$

$$R_{C3}=\frac{\frac{\hat{\kappa}_T}{\hat{h}}+\frac{1}{\hat{h}^2}}{\Omega_5+\Omega_6} \quad \text{... [36]}$$

Here,

$$\Omega_1=\left(\varepsilon\Psi_4+\frac{\varepsilon^2}{2}\Psi_5+\frac{\varepsilon^3}{3}\Psi_6+\frac{\varepsilon^4}{4}\Psi_7+\frac{\mathrm{Sinh}(\eta_1\varepsilon)}{\eta_1}\Psi_8+\left(\frac{\mathrm{Cosh}(\eta_1\varepsilon)-1}{\eta_1}\right)\Psi_9+\frac{\hat{\kappa}_T\varepsilon^5}{120\hat{h}}\right)$$

$$\Omega_2=\left(\frac{\varepsilon_m^2}{2}\Psi_2+\left(\frac{\mathrm{Sinh}(\eta_2\varepsilon_m)}{\eta_2^3}-\frac{\varepsilon_m}{\eta_2^2}-\frac{\varepsilon_m^3}{6}\right)\Delta_1+\frac{\mathrm{Cosh}(\eta_2\varepsilon_m)\Psi_1}{\eta_2}\right)$$

$$\Omega_3=\left(\begin{array}{l}\varepsilon\Psi_4+\left(\frac{1-(1-\varepsilon)^2}{2}\right)\Psi_5+\left(\frac{1-(1-\varepsilon)^3}{3}\right)\Psi_6+\left(\frac{1-(1-\varepsilon)^4}{4}\right)\Psi_7+\frac{\hat{\kappa}_T}{\hat{h}}\left(\frac{1-(1-\varepsilon)^5}{120}\right)\\ \left(\frac{\mathrm{Sinh}(\eta_1)}{\eta_1}-\frac{\mathrm{Sinh}(\eta_1(1-\varepsilon))}{\eta_1}\right)\Psi_8+\left(\frac{\mathrm{Cosh}(\eta_1)}{\eta_1}-\frac{\mathrm{Cosh}(\eta_1(1-\varepsilon))}{\eta_1}\right)\Psi_9\end{array}\right)$$

$$\Omega_4=\left(\begin{array}{l}\left(\frac{1-(1-\varepsilon_m)^2}{2}\right)\Psi_2+\left(\frac{\mathrm{Sinh}(\eta_2)-\mathrm{Sinh}(\eta_2(1-\varepsilon_m))}{\eta_2^3}-\frac{\varepsilon_m}{\eta_2^2}-\left(\frac{1-(1-\varepsilon_m)^3}{6}\right)\right)\Delta_1+\\ \left(\frac{\mathrm{Cosh}(\eta_2)-\mathrm{Cosh}(\eta_2(1-\varepsilon_m))}{\eta_2}\right)\Psi_1\end{array}\right)$$

$$\Omega_5=\left(\Psi_4+\varepsilon\Psi_5+\varepsilon^2\Psi_6+\varepsilon^3\Psi_7+\mathrm{Cosh}(\eta_1\varepsilon)\Psi_8+\mathrm{Sinh}(\eta_1\varepsilon)\Psi_9+\frac{\hat{\kappa}_T\varepsilon^4}{24\hat{h}}\right)$$

$$\Omega_6=\left(\varepsilon_m\Psi_2+\left(\frac{\mathrm{Cosh}(\eta_2\varepsilon_m)}{\eta_2^2}-\frac{1}{\eta_2^2}-\frac{\varepsilon_m^2}{2}\right)\Delta_1+\mathrm{Sinh}(\eta_2\varepsilon_m)\Psi_1\right)$$

4.0 Results and Discussion

Analytical investigation into the influence of HTG, CTG, and STG on the onset of Rayleigh- Darcy convection of couple stress fluid in a composite system. The graphs illustrate the fluctuation of the critical Rayleigh number as a function of thermal depth for different values of couple stress parameter (C_p), depth ratio ($\hat{h}$), Darcy number (Da), thermal diffusivity ratio ($\hat{\kappa}_T$) , thermal depth in porous medium (ε_m), and couple stress viscosity ratio ($\hat{\Lambda}$).

We fix the values of the dimensionless parameters that are viscosity ratio $\hat{\mu} = 1$, and thermal expansion coefficient ratio $\hat{\beta} = 1$. Here, R_{c1}, R_{c2} and R_{c3} represent the respective the critical Rayleigh number for HTG, CTG, and STG, respectively.

The Figure *A*1, demonstrates the variation of R_{c1}, R_{c2} and R_{c3} as a function of thermal depth (ε) for HTG, CTG and STG. For the fixed parameters $C_p = 0.5$, $Da = 0.003$, $\varepsilon_m = 0.5$, $\hat{h} = 1$, $\hat{\kappa}_T = 1$, $\hat{\Lambda} = 1$. The graph demonstrates that the curve for HTG declines for the thermal depth $0 \le \varepsilon \le 0.4$ and for the thermal depth $0.6 \le \varepsilon \le 1$ increases. Here, RDC destabilizes at smaller thermal depths but stabilizes at greater thermal depths. With CTG, the curve declines with increasing thermal depth, rendering RDC unstable. In contrast, the STG curve increases with increasing thermal depth, hence stabilizing RDC. By establishing an appropriate thermal gradient, the onset of RDC in composite systems can be controlled.

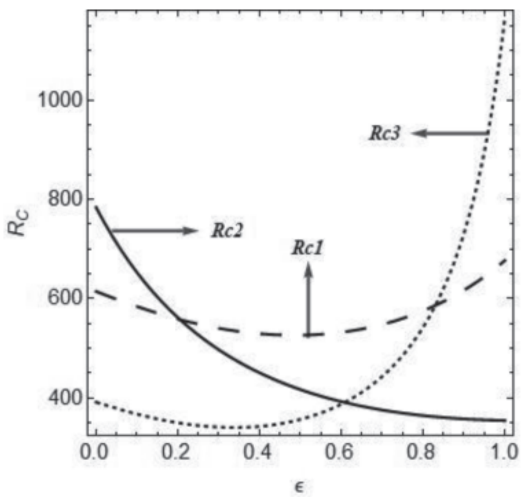

Figure: A1, The cumulative influence of HTG, CTG, and STG

In figure: *A*2(*a*, *b*, *c*) illustrates the deviance of R_{c1}, R_{c2} and R_{c3} as a function of thermal depth (ε) for HTG, CTG and STG. For the fixed parameters $Da = 0.003$, $\varepsilon_m = 0.5$, $\hat{h} = 1$, $\hat{\kappa}_T = 1$, $\hat{\Lambda} = 1$, $\hat{\mu} = 1$, $\hat{\beta} = 1$, and varying the couple stress parameter $Cp = 0.4$, $Cp = 0.6$, $Cp = 0.8$. From the graph, we notice that R_{c1}, R_{c2} and R_{c3} elevates as the value of Cp increases for HTG, CTG and STG. As a result, the rise in Cp delays RDC, this ultimately results in the system becoming more stable.

In Figure: *A*3 (*a*, *b*, *c*) depicts the variation of R_{c1}, R_{c2} and R_{c3} as a function of thermal depth (ε) for HTG, CTG and STG. For the fixed parameters $Da = 0.003$, $\varepsilon_m = 0.5$, $\hat{h} = 1$, $\hat{\kappa}_T = 1$, $Cp = 0.5$, $\hat{\mu} = 1$, $\hat{\beta} = 1$, and varying the couple stress viscosity ratio $\hat{\Lambda} = 0.5$, $\hat{\Lambda} = 0.7$, $\hat{\Lambda} = 1.0$ from the graph, we notice that R_{c1}, R_{c2} and R_{c3} elevates as the value of $\hat{\Lambda}$ increases for HTG, CTG and STG. As a result, the rise in $\hat{\Lambda}$ delays RDC, this ultimately results in the system becoming more stable.

In figure: A4(*a*, *b*, *c*) depicts the variation of R_{c1}, R_{c2} and R_{c3} as a function of thermal depth (ε) for HTG, CTG and STG. For the fixed parameters $\hat{\Lambda} = 1.0$, $\varepsilon_m = 0.5$, $\hat{h} = 1$, $\hat{\kappa}_T = 1$, $Cp = 0.5$, $\hat{\mu} = 1$, $\hat{\beta} = 1$, and varying the Darcy number $Da = 0.003$, $Da = 0.005$, and $Da = 0.007$. From the figure we observe that R_{c1}, R_{c2} and R_{c3} declines as Da value increases for HTG, CTG and STG. Hence, the increase in Da accelerates RDC and consequently weakens the system.

In figure: *A*5(*a*, *b*, *c*) depicts the variation of R_{c1}, R_{c2} and R_{c3} as a function of thermal depth (ε) for HTG, CTG and STG. For the fixed parameters $\hat{\Lambda} = 1.0$, $\varepsilon_m = 0.5$, $\hat{h} = 1$, $Da = 0.003$, $Cp = 0.5$, $\hat{\mu} = 1$, $\hat{\beta} = 1$, and varying the Darcy number $\hat{\kappa}_T = 0.6$, $\hat{\kappa}_T = 0.8$, and $\hat{\kappa}_T = 1.0$. From the figure we observe that R_{c1}, R_{c2} and R_{c3} declines as $\hat{\kappa}_T$ value increases for HTG, CTG and STG. Hence, the increase in system. $\hat{\kappa}_T$ accelerates RDC and consequently weakens the system.

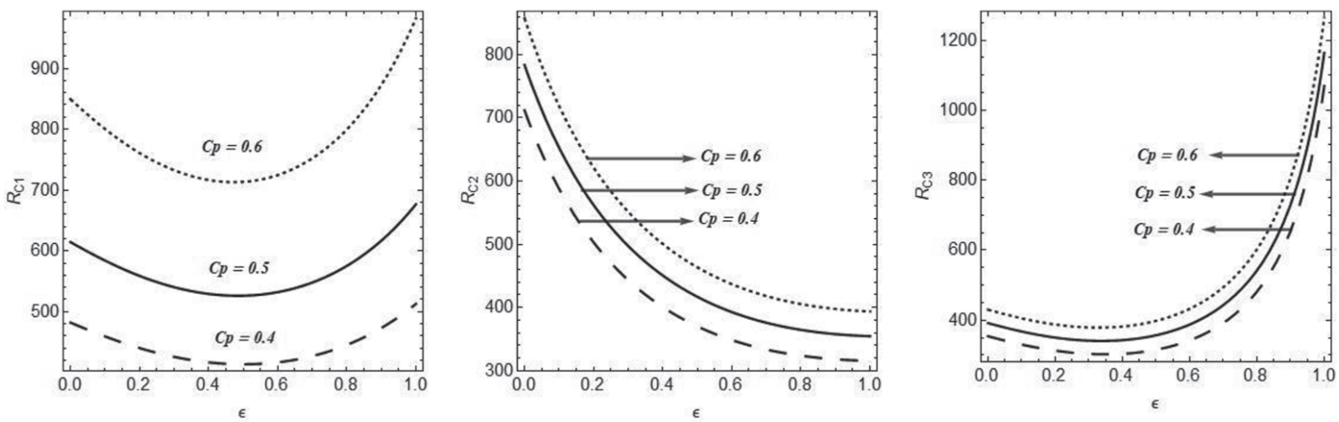

Figure: *A*2 (*a*, *b*, *c*), Effect of *Cp* in the cases of HTG, CTG and STG

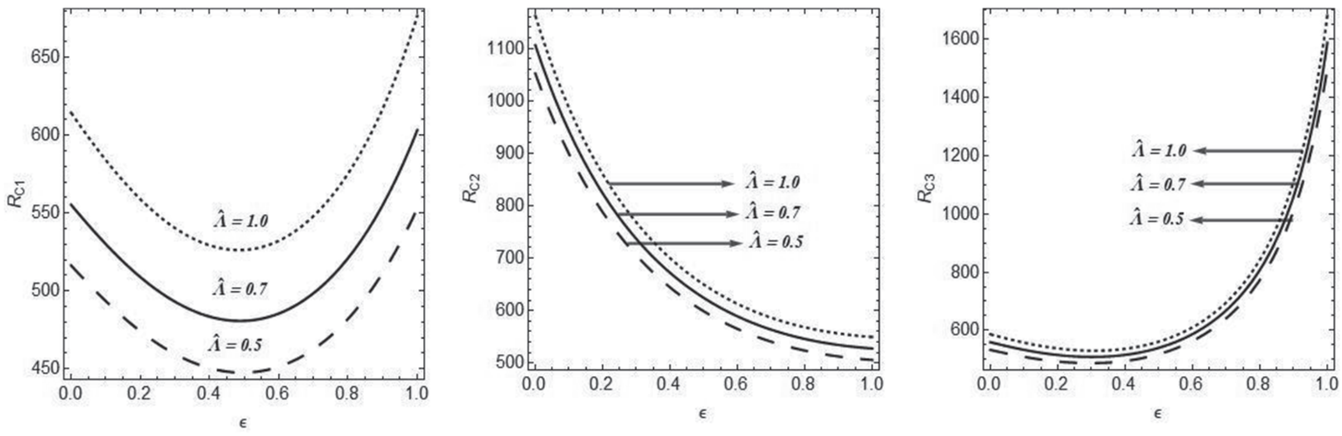

Figure: ***A*3** (*a*, *b*, *c*), Effect of $\hat{\Lambda}$ in the cases of HTG, CTG and STG

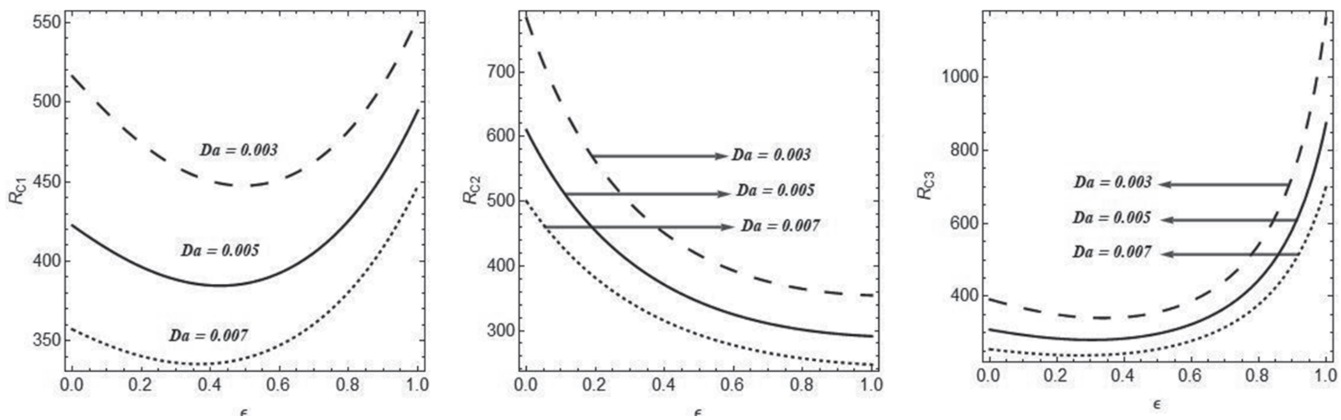

Figure: ***A*4** (*a*, *b*, *c*), Effect of *Da* in the cases of HTG, CTG and STG

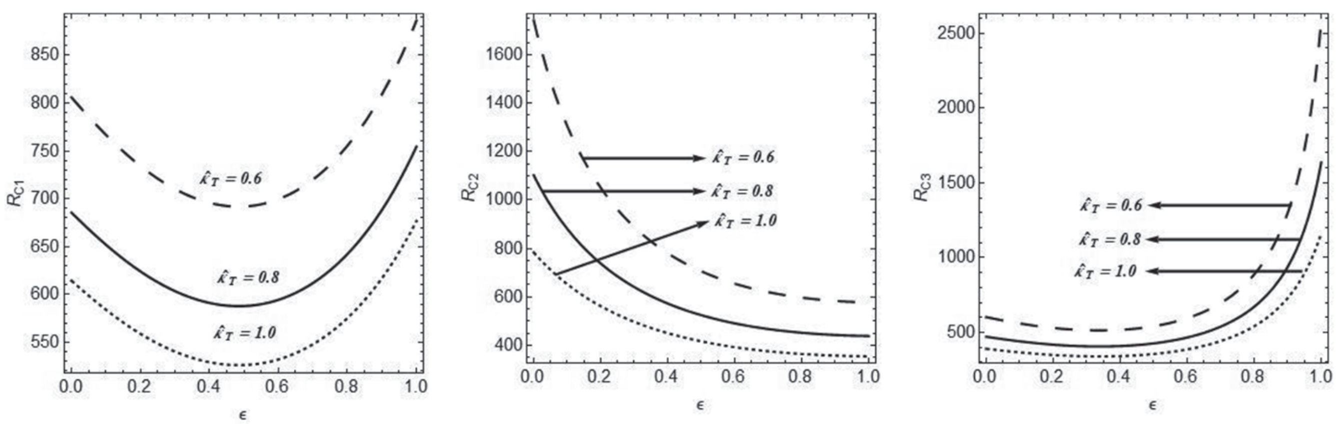

Figure: A5 (*a*, *b*, *c*), Effect of $\hat{\kappa}_T$ in the cases of HTG, CTG and STG

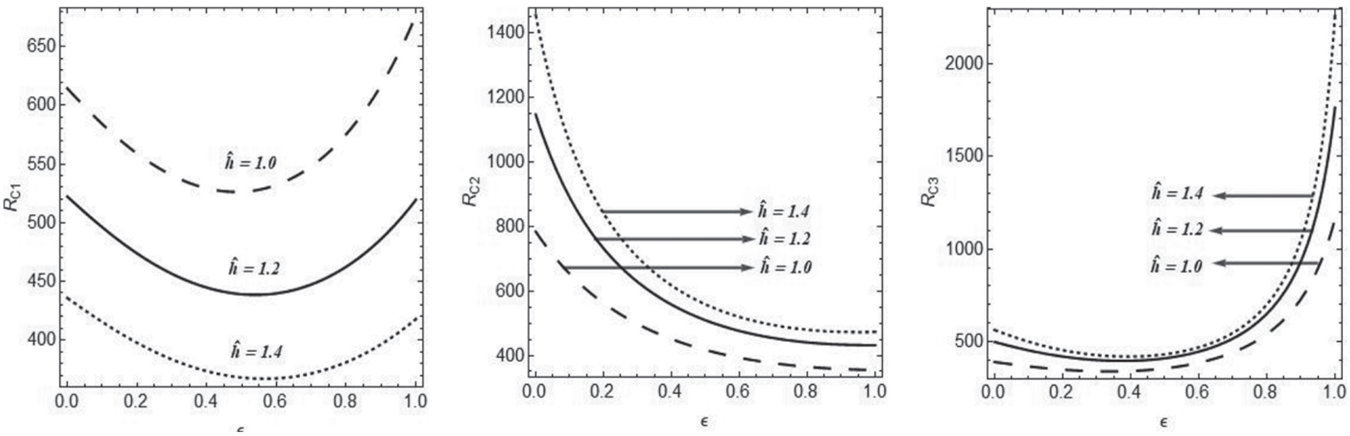

Figure: ***A6*** (a, b, c), Effect of $\hat{h}$ in the cases of HTG, CTG and STG

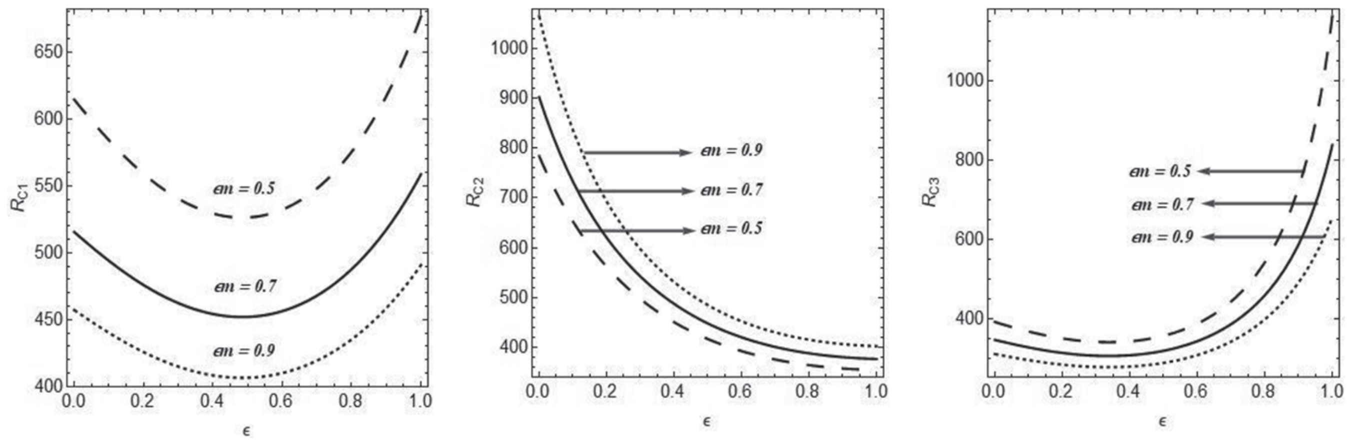

Figure: ***A7*** (*a*, *b*, *c*) , Effect of ε_m in the cases of HTG, CTG and STG

In Figure: *A*6(*a*, *b*, *c*) depicts the variation of R_{c1}, R_{c2} and R_{c3} as a function of thermal depth (ε) for HTG, CTG and STG. For the fixed parameters $\hat{\Lambda} = 1.0$, $\varepsilon_m = 0.5$, $Da = 0.003$, $\hat{\kappa}_T = 1$, $Cp = 0.5$, $\hat{\mu} = 1$, $\hat{\beta} = 1$, and varying the depth ratio $\hat{h} = 1$, $\hat{h} = 1.2$, and $\hat{h} = 1.4$. From the figure we observe that R_{c1} declines as $\hat{h}$ value increases for HTG. Hence, the increase in $\hat{h}$ accelerates RDC and consequently weakens the system. Whereas in the case of CTG and STG we observe that R_{c2} and R_{c3} accelerates as $\hat{h}$ value increases. Hence, the increase in $\hat{h}$ delays RDC and consequently strengthens the system.

In figure: *A*7(*a*, *b*, *c*) depicts the variation of R_{c1}, R_{c2} and R_{c3} as a function of thermal depth (ε) for HTG, CTG and STG. For the fixed parameters $\hat{\Lambda} = 0.5$, $Da = 0.003$, $\hat{h} = 1$, $\hat{\kappa}_T = 1$, $Cp = 0.5$, $\hat{\mu} = 1$, $\hat{\beta} = 1$, and varying the thermal depth in porous medium $\varepsilon_m = 0.5$, $\varepsilon_m = 0.7$ and $\varepsilon_m = 0.9$. From the figure we observe that R_{c1} and R_{c3} declines as ε_m value increases for HTG and STG. Hence, the increase in ε_m accelerates RDC and consequently weakens the system. Whereas in the case of CTG we observe that R_{c2} accelerates as ε_m value increases. Hence, the increase in ε_m delays RDC and consequently strengthens the system.

5. Conclusion

The following are the analysis's conclusions:

- The thermal depth of the fluid layer substantially influences the beginning of RDC.

For $\varepsilon < 0.2$ we have $Rc_2 > R_{c1} > R_{c3}$, that is CTG is most stable.

For $0.2 < \varepsilon < 0.6$ we have $Rc_1 > R_{c2} > R_{c3}$, that is HTG is most stable.

For $0.6 < \varepsilon < 0.8$ we have $Rc_1 > R_{c3} > R_{c2}$, that is HTG is most stable.

For $0.8 < \varepsilon < 0.6$ we have $Rc_3 > R_{c1} > R_{c2}$, that is HTG is most stable.

- Larger values of Couple stress parameter Cp and couple stress viscosity ratio $\hat{\Lambda}$ and smaller values of Darcy number Da govern RDC in a couple stress fluid composite system for all temperature gradients.
- In the case of HTG, RDC is delayed by lower levels of $\hat{h}$, ε_m, and $\hat{\kappa}_T$. In the context of CTG, greater values of $\hat{h}$, ε_m, and $\hat{\kappa}_T$ delay RDC. In the case of STG, greater values of $\hat{h}$ delaying RDC.

References

[1] Nield, D. A., and Bejan, A., "Convection in porous media". *Springer-Verlag New York Inc*, (1999).

[2] Sun, W. J., "Convective instability in superposed porous and free layers". Ph.D. dissertation, University of Minnesota, Minneapolis, (1973).

[3] Nield, D. A., "Onset of convection in a fluid layer overlying a layer of a porous medium", *J. Fluid Mech.*, 81, pp. 513–522, (1977).

[4] Beckermann, C., Ramadhyani, S., and Viskanta, R., "Natural convection flow and heat transfer between a fluid layer and a porous layer inside a rectangular enclosure." *J. Heat Trans.*, 109, pp. 363–370, (1987).

[5] Chen F. and C. F. Chen, "Convection in superposed fluid and porous layers," *J. Fluid Mech.*, 234, 97-119 (1992).

[6] Robert McKibbian "Anisotropic modelling of thermal convection in multilayered porous media" *J. Fluid Mech.*, vol. 118, pp. 315-339, Printed in Great Britain 315, (1982).

[7] Jamet, D., Chandesris, M., and Goyeau, B., "On the equivalence of the discontinuous one- and two-domain approaches". T*rans. Porous Med.*, 78, p. 403-418, (2009).

[8] Chang, M., "Thermal convection in superposed fluid and porous layers subjected to a plane poiseuille flow", *Physics of Fluids*, 18(3), pp. 1–7, (2006).

[9] Hill, A. A., and Straughan, B., "Poiseuille flow in a fluid overlying a porous medium", *J. Fluid Mech.*, 603, pp. 137–149, (2008).

[10] Hirata, S. C., Goyeau, B., Gobin, D., and Cotta, R. M., "Stability in natural convection in superposed fluid and porous layers using integral transforms". *Num. Heat Trans.*, 50(5), pp. 409–424, (2006).

[11] Hirata, S. C., Goyeau, B., Gobin, D., Chandesris, M., and Jamet, D., "Stability of natural convection in superposed fluid and porous layers: equivalence of the one-and two-domain approaches", *Int. J. Heat Mass Trans.*, 52(1-2), pp. 533–536, (2009).

[12] Beavers, G. S., and Joseph, D. D., 1967. "Boundary conditions at a naturally permeable wall", *J. Fluid Mech.*, 30, pp.197–207, (1967).

[13] Alberto Ochoa-Tapia J., Stephen Whitaker, "Momentum transfer at the boundary between a porous medium and a homogeneous fluid—I. Theoretical development", *International Journal of Heat and Mass Transfer*, Volume 38, Issue 14, Pages 2635-2646, (1995).

[14] Vafai K and Thiyagaraja R, "Analysis of flow and heat transfer at the interface region of a porous medium", *International Journal of Heat and Mass Transfer* Volume 30, Issue 7, 1391-1405, (1987).

[15] Alazmi, B., and Vafai, K., "Analysis of fluid flow and heat transfer interfacial conditions between a porous medium and a fluid layer", *International Journal of Heat and Mass Transfer*, 44(9), 1735–1749, (2001).

[16] Sumithra R. and Manjunatha.N, "Effects of parabolic and inverted parabolic temperature profiles on magneto Marangoni convection in a composite layer", *International Journal current Research*, 6, 5435-5450, (2014).

[17] Sumithra, R., Vanishree, R. K., & Manjunatha, N., "Effect of constant heat source/sink on single component Marangoni convection in a composite layer bounded by adiabatic boundaries in presence of uniform & non uniform temperature gradients", *Malaya Journal of Matematik*, 8(2), 306–313, (2020).

[18] Stokes V.K. "Couple stresses in fluids", Phys. Fluids, 9 1709-1716, (1966).

[19] Sharma R. C. and Shivani Sharma, "Couple-stress fluid heated from below in porous medium", *Indian Journal of Physics*, 75B (2), 137-139, (2001).

[20] Malashetty M. S. and D. Basavaraja, "Effect of JOURNAL OF MINES, METALS & FUELS 11 thermal/gravity modulation on the onset of Rayleigh-Benard convection in a couple stress fluid", International Journal of Transport Phenomena, vol. 7, pp. 31–44, (2005).

[21] Rudraiah, N., Veerapa, B., Balachandra, R.S: "Effects of non-uniform thermal gradient and

adiabatic boundaries on convection in porous media", *Journal of Heat Transfer*, 102, 254, (1980).

[22] Shivakumara, I. S., Sureshkumar, S., & Devaraju, N., "Effect of non-uniform temperature gradients on the onset of convection in a couple-stress fluid-saturated porous medium", Journal of Applied Fluid Mechanics, 5(1):49-55, (2012).

[23] Shankar B.M., Shivakumara I.S., Chiu-On Ng., "Stability of couple stress fluid flow through horizontal porous layer", *Journal of Porous Media*, 19, 5, pp.391-404, (2016).

[24] P.G. Siddheshwar and S. Pranesh, "Effect of a non-uniform basic temperature gradient on Rayleigh-Benard convection in a micropolar fluid", *International Journal of Engineering Science*, vol.36, 11, 1183–1196, (1998).

[25] Shivakumara I.S., "Onset of convection in a couple-stress fluid saturated porous medium: Effects of non-uniform temperature gradients", *Archive of Applied Mechanics*, Vol.80, No.8, pp.949-957, (2010).

[26] Sumithra, R., and Selvamary, T. A., "Single component Darcy-Benard surface tension driven convection of couple stress fluid in a composite layer", *Malaya Journal of Matematik* (MJM), 9(1, 2021), 797–804, (2021).